

Functional organic nanotubes from hollow helical scaffolds

Anzar Khan, Stefan Hecht*

Institut für Chemie/Organische Chemie, Freie Universität Berlin, Takustr. 3, 14195 Berlin, Germany

Received 5 April 2004; received in revised form 19 April 2004; accepted 21 April 2004

Available online 22 October 2004

Abstract

A conceptually new approach to organic nanotubes has been developed that in principle allows for control over the tube's dimensions as well as location of interior and exterior surface functionalities. Our approach is based on the folding of a suitable polymer backbone into a defined hollow helical conformation followed by intramolecular crosslinking to lock the tubular structure. Subsequent postfunctionalization should give access to modularly functionalized tubular nanoobjects with potential application in molecular scale devices and smart materials. Here, we describe the initial proof of principle for our concept.

© 2004 Elsevier B.V. All rights reserved.

Keywords: Helical scaffold; Tubular nanoobjects; Postfunctionalization

1. Introduction

The emerging nanotechnology era is largely driven by the prospect of revolutionary device miniaturization, whereby implementation of individual molecule-sized components promises an enormous increase in packing density of circuitry [1]. Chemistry as “the original synthetic nanotechnology” [2] is playing a key role in this so-called bottom-up approach [3] for which a set of molecular building blocks with a variety of shapes and functions is needed. Tubular nanoobjects constitute important components of such construction kit because of their inherent geometric features that differentiate between defined inner and outer surfaces as well as termini. While the cylindrical dimensionality allows for directionality that is needed for transport processes, the spatial segregation encodes addressability needed for self-assembly into more complex architectures [4–6] or provides handles for rational manipulation [7,8]. Carbon [9] and inorganic nanotubes [10] are certainly very promising in view of future molecular electronics as well as materials applications. While many fascinating properties have been revealed and exploited in first devices, these structures still suffer from significant

drawbacks related to their synthesis (control over length and structural type) [11] and peripheral modification (control over location of surface functionality) [12,13]. Inspired by natural design concepts, several molecular based approaches to obtain organic nanotubes have been developed and promise a superior control over structure and local functionality [14,15]. Most of the strategies explored thus far have taken advantage of a combination of covalent and non-covalent synthesis based on various structural motifs including hollow or self-assembled helices, stacked macrocycles and rosettes, cylindrical micelles and rolled bilayer sheets.

Our group has recently described a conceptually new approach (Fig. 1) to generate organic nanotubes on the basis of intramolecularly crosslinked, helically folded polymers [16]. Thereby, polymerization of suitable functional monomers leads to a polymer strand (primary structure) that is folding into an ordered helical conformation containing an inner void (secondary structure), which after covalent stabilization using intramolecular crosslinking yields the rigid organic nanotube. Subsequent inner and outer postfunctionalization should afford nanochannels or insulated nanowires with defined surface functionality and controlled dimension. These advanced nanoobjects are potentially interesting building blocks for the construction of new materials and devices.

* Corresponding author. Tel.: +49 30 838 52451; fax: +49 30 838 52551.
E-mail address: shecht@chemie.fu-berlin.de (S. Hecht).

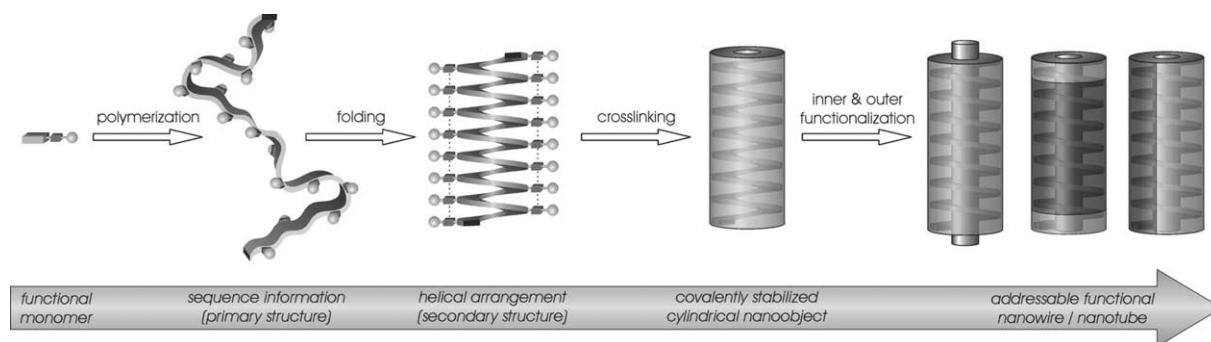


Fig. 1. Functional organic nanotubes via intramolecular crosslinking of helically folded polymer backbones followed by inner/outer postmodification.

Our approach takes advantage of the power of covalent chemistry to yield a defined oligomer/polymer sequence and enhance the object's stability by crosslinking, while utilizing non-covalent interactions to drive the formation of the helical structure without defects. It should be noted that our strategy allows for unprecedented control over surface functionality as well as length control (in principle). Furthermore, the inherent chirality of the helical scaffold should provide the nanotubes with additional advantageous properties. Here, we briefly discuss the initial investigations into the feasibility of our concept that serve as a first proof of concept and have been published recently [16].

2. Experimental

2.1. General methods

3,5-Diiodobenzaldehyde was prepared from ethyl 4-aminobenzoate in a four-step sequence involving iodination, deamination, reduction followed by oxidation as described in the literature [17]. Pd(PPh₃)₄ was freshly prepared [18], all other chemicals were commercial and used as received. THF and acetonitrile were distilled prior to use under N₂ atmosphere over sodium/benzophenone ketyl and calcium hydride, respectively. Column chromatography was carried out with 130–400 mesh silica gel. NMR spectra were recorded on Bruker AB 250 (250.1 and 62.9 MHz for ¹H and ¹³C, respectively) and AC500 as well as Delta JEOL Eclipse 500 (500 and 126 MHz for ¹H and ¹³C, respectively) spectrometers at 23 ± 2 °C using residual protonated solvent signal as internal standard (¹H: δ(CHCl₃) = 7.24 ppm, δ(DMSO) = 2.49, δ(CH₃CN) = 1.94 ppm and ¹³C: δ(CHCl₃) = 77.0 ppm, δ(DMSO) = 39.7 ppm). Mass spectrometry was performed on Perkin-Elmer Varian Type MAT 771 and CH6 (EI), Type CH5DF (FAB), or Bruker Reflex with 337 nm laser excitation (MALDI-TOF) instruments. Elemental analyses were performed on a Perkin-Elmer EA 240. GPC measurements were performed on a Waters 515 HPLC pump-GPC system equipped with a Waters 2487 UV detector (254 nm detection wavelength) using THF as the mobile phase at 40 °C and a

flow rate of 1 mL/min. The samples were separated through Waters Styragel HR1 or HR3 columns with 5 μm bead sizes. The columns were calibrated with several narrow polydispersity polystyrene samples and toluene served as internal standard. The HPLC system consisted of a Knauer Eurosphere 7 μm C18, 4 mm × 120 mm silica gel column and UV-detection at 254 nm with an eluent flow of 1 mL/min.

2.2. Optical spectroscopy

UV–vis absorption and fluorescence emission/excitation spectra were recorded in various solvents of spectroscopic grade using quartz cuvettes of 1 cm path length on a Cary 50 Spectrophotometer and a Cary Eclipse Fluorescence Spectrophotometer, respectively, both equipped with Peltier thermostated cell holders (Δ*T* = ±0.05 °C). Unless stated otherwise, all experiments were carried out at 25 ± 0.05 °C. For fluorescence measurements, the samples were not degassed since comparison of degassed with non-degassed solutions did not show measurable differences within the error of the experiment. The samples were excited at λ_{exc} = 290 nm, slit widths were set to 2.5 nm bandpass for excitation and 5 nm bandpass for emission. Fluorescence spectra were corrected for variations in photomultiplier response over wavelength using correction curves generated on the instrument. For titration experiments, stock solutions in CHCl₃ and CH₃CN with optical densities OD(λ_{max}) ~ 0.8 for UV–vis absorption and OD(λ_{max}) ~ 0.1 for fluorescence measurements were used to prepare samples with varying solvent composition. The corrected fluorescence spectra were normalized by the exact OD_{290 nm}.

2.3. 3,5-Diiodocinnamic acid **1**

3,5-Diiodobenzaldehyde (1.07 g, 3 mmol), malonic acid (0.31 g, 3 mmol), piperidine (1 mL), DMF (8 mL), glacial acetic acid (1 mL), and acetic anhydride (1.5 mL) were suspended in toluene (10 mL) and heated overnight at 120 °C. Then, water (30 mL) was added and it was refluxed for 1 h. The formed white solid was isolated by filtration and washed with water to afford the crude acid that can be further purified by recrystallization from ethanol furnishing

0.70 g of a white solid (56% yield). ^1H NMR (250 MHz, DMSO- d_6 , $23 \pm 2^\circ\text{C}$): δ 8.08 (broad s, 3H, Ar-H), 7.42 (d, 3J (H, H) = 16.4 Hz, ^1H , C=CH–), 6.61 (d, 3J(H, H) = 16.4 Hz, ^1H , C=CH–); ^{13}C NMR (125 MHz, DMSO- d_6 , $23 \pm 2^\circ\text{C}$): δ 172.17, 150.47, 145.86, 143.58, 140.95, 127.20, 101.57; EI-MS (80 eV, 100°C): m/z = 400.0 (Calcd. 399.9 for $\text{C}_9\text{H}_6\text{I}_2\text{O}_2^+$); Anal. C: 26.87, H: 1.19 (Calcd. C: 27.03, H: 1.51).

2.4. 2-[2-(2-Methoxy-ethoxy)-ethoxy]-ethyl 3,5-diiodocinnamate **2**

Crude acid **1** (4.60 g, ~ 11.5 mmol) was mixed with thionyl chloride (15 mL), three drops of DMF added, and it was heated at 60°C for 2 h. Excess thionyl chloride was evaporated and the remaining compound dried on a vacuum pump for 3 h to afford the crude acid chloride as a light brownish solid. Triethylene glycol monomethyl ether (2.7 mL, 17.25 mmol), triethylamine (3.2 mL, 23.0 mmol), and 4-dimethylaminopyridine (DMAP; 0.14 g, 1.15 mmol) were dissolved in CH_2Cl_2 (10 mL), the solution cooled to 0°C (ice bath), a solution of the acid chloride in CH_2Cl_2 (30 mL) slowly added over a period of 30 min, the resulting reaction mixture allowed to warm to rt and stirred overnight. Filtration followed by washing of the filtrate with sat. aqueous NH_4Cl and brine, drying over MgSO_4 , evaporation of the solvent, and column chromatography (40% ethyl acetate in hexane, R_f = 0.2) gave 4.136 g of the product as slightly yellow oil ($\sim 66\%$ yield). ^1H NMR (500 MHz, CDCl_3 , $23 \pm 2^\circ\text{C}$): δ 8.01 (t, 4J (H, H) = 1.5 Hz, ^1H , Ar-H), 7.77 (d, 4J (H, H) = 1.5 Hz, 2H, Ar-H), 7.44 (d, 3J (H, H) = 16.0 Hz, ^1H , C=CH–), 6.40 (d, 3J (H, H) = 16.0 Hz, ^1H , C=CH–), 4.33 (t, 3J (H, H) = 4.8 Hz, 2H, $\text{CO}_2\text{--CH}_2$), 3.74 (t, 3J (H, H) = 4.8 Hz, 2H, O– CH_2), 3.68–3.62 (m, 6H, O– CH_2), 3.53 (t, 3J (H, H) = 4.8 Hz, 2H, O– CH_2), 3.35 (s, 3H, O– CH_3); ^{13}C NMR (125 MHz, CDCl_3): δ 165.95, 146.30, 141.47, 138.08, 135.97, 120.53, 71.92, 70.62, 70.58, 69.09, 63.94, 59.04; EI-MS (80 eV, 150°C): 546.1 (M^+ , 21%), 501 ($M - \text{C}_2\text{H}_5\text{O}^+$, 6%), 427 ($M - \text{C}_5\text{H}_{11}\text{O}_3^+$, 100%), 383 ($M - \text{C}_7\text{H}_{15}\text{O}_4^+$, 80%), 256 ($M - \text{C}_5\text{H}_{11}\text{O}_3\text{I}^+$, 61%); 6EI-HRMS: m/z = 545.94333 (Calcd. 545.94000 for $\text{C}_{16}\text{H}_{20}\text{O}_5\text{I}_2^+$), 426.86577 (Calcd. 426.86920 for $\text{C}_{11}\text{H}_9\text{O}_2\text{I}_2^+$), 382.84455 (Calcd. 382.84299 for $\text{C}_9\text{H}_5\text{OI}_2^+$); Anal. C: 35.29, H: 3.39 (Calcd. C: 35.19, H: 3.69); HPLC (90% MeOH in H_2O , 1 mL/min): 99.0% peak area.

2.5. Poly(*m*-aryleneethynylene) **3**

Monomer **2** (546 mg, 1 mmol), CuI (15 mg, 0.08 mmol), and $\text{Pd}(\text{PPh}_3)_4$ (69 mg, 0.06 mmol) were loaded in a flame dried 10 mL Schlenk tube, which was evacuated and refilled with argon. Dry and degassed acetonitrile (4 mL) was submitted to the tube via syringe, 1,8-diazabicyclo[5.4.0]undec-7-ene (DBU; 0.9 mL, 6 mmol) and trimethylsilylacetylene (TMSA; 142 μL , 1 mmol) were added immediately followed

by addition of distilled H_2O (18 μL , 1 mmol). The tube was covered with aluminum foil and the reaction mixture was allowed to stir at rt for 3 days after which it was precipitated in ether (500 mL). The resulting polymer was redissolved in CH_2Cl_2 and passed through a short column of silica gel to give ~ 250 mg of **3** as a greyish powder ($\sim 79\%$ yield). ^1H NMR (500 MHz, CDCl_3 , $23 \pm 2^\circ\text{C}$): δ 7.68–7.62 (broad m, 4H, Ar-H, C=CH), 6.53 (broad d, 3J (H,H) = 15.7 Hz, 1H, C=CH), 4.35 (broad t, 2H, $\text{CO}_2\text{--CH}_2$), 3.75 (broad t, 2H, O– CH_2), 3.67–3.62 (broad m, 6H, O– CH_2), 3.52 (broad t, 2H, O– CH_2), 3.34 (broad s, 3H, O– CH_3); ^{13}C NMR (125 MHz, CDCl_3): δ 166.40, 142.90, 135.82, 135.35, 131.13, 124.07, 120.16, 89.21, 77.04, 70.73, 69.24, 63.99, 59.10; IR (KBr): 3434, 2923, 2853, 1716, 1641, 1593, 1288, 1177, 1106 cm^{-1} ; Anal. C: 69.91/69.52, H: 7.75/8.22 (Calcd. for $(\text{C}_{18}\text{H}_{20}\text{O}_5)_n$ C: 68.34, H: 6.37); GPC (THF, 40°C): $M_w = 24\,700$, $M_n = 18\,400$, PDI (M_w/M_n) = 1.34; UV–vis (CHCl_3 , 25°C) λ_{max} (abs/conc) 292 nm (0.581/70.6 mg/L).

2.6. Irradiation of Poly(*m*-aryleneethynylene) **3**

Preparative irradiations were performed using a Philips HPK 125 W high-pressure mercury lamp equipped with a water-cooled photoreactor of Duran[®] (pyrex) glass ($\lambda_{5\%T} = 316$ nm). The solutions (10 mg polymer **3**/100 mL CH_3CN , $\sim 7 \times 10^{-6}$ M) were degassed with nitrogen for 10 min, continuously irradiated, and samples for GPC and UV–vis taken at given time intervals. For ^1H NMR spectra, the solvent was evaporated at a given time, the sample thoroughly dried on a vacuum pump, and redissolved in CDCl_3 .

3. Results and discussion

3.1. Backbone synthesis

The needed polymer backbone has to contain all necessary information and functionality in order to: (i) fold in a reversible fashion into a hollow helical structure in which the non-neighboring crosslinking groups are located in close proximity, (ii) specific residues are exposed at the inner and outer surfaces to allow for postfunctionalization, (iii) all chemical processes can be carried out independently, i.e. they are orthogonal to one another. These stringent requirements exclude most known helical foldamers [19] and polymers [20,21] since most of these compounds do not contain an inner void and their high pitch hinders efficient crosslinking due to large side chain separation. On the contrary, Moore's amphiphilic oligo (*meta*-phenyleneethynylene)s [22] offer several advantages since they contain a significant inner void (assuming a 6-helix [23] yields an available inner cavity measuring ~ 0.7 nm in diameter), allow for the introduction of multiple crosslinks per turn, position the reactive groups in close proximity (π,π -stacking distance of neighboring units in adjacent turns), and exhibit a well-characterized confor-

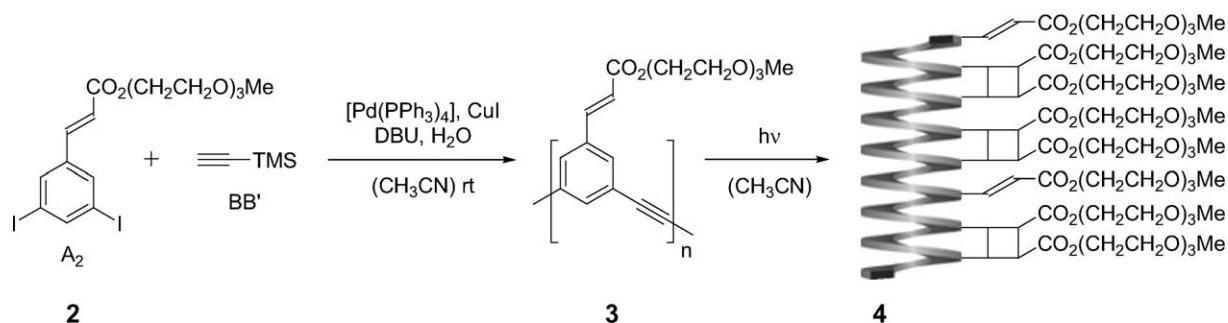


Fig. 2. Synthesis and crosslinking of amphiphilic poly(*m*-phenyleneethynylene) **3**.

mational behavior that can easily be monitored using UV–vis absorption and fluorescence spectroscopies.

Therefore, amphiphilic poly(*meta*-phenyleneethynylene)s [24] were chosen as the backbone in our initial experiments while the reactive groups were incorporated as cinnamates to utilize [2+2]photodimerization reactions for intramolecular crosslinking. We employed our recently developed $A_2 + BB'$ polycondensation route [25] to prepare poly(*m*-phenyleneethynylene) **3** (Fig. 2) having a respectable number average degree of polymerization ($DP \sim 60$) and a typical polydispersity index ($PDI = 1.3$). The diiodocinnamate monomer **2** was synthesized from known 3,5-diiodobenzaldehyde [17] in two steps involving a Knoevenagel-type condensation followed by esterification with triethylene glycol monomethyl ether. Most importantly, comparison of the ^{13}C NMR spectra of **3** with literature values of diacetylene oligomers, almost exactly resembling the investigated polymer repeat units [26], clearly shows the absence of detrimental diyne defects in the polymers (**3**) prepared by our method.

3.2. Backbone folding

Helix formation in polar solvents, such as acetonitrile, is guided by the *meta*-connectivity as well as facile π, π -stacking between electron-deficient aromatic units [27] and is entropically driven by solvophobic interactions leading to exposure of the polar side chains while hiding the non-polar aromatic backbone. To monitor the helix-coil transition both UV–vis spectroscopy taking advantage of different absorptions of *transoid* and *cisoid* conformations [22] as well as fluorescence spectroscopy discriminating between emission from isolated (cross-conjugated) and stacked “pseudoexcimer”-like repeat units [28] can be used. Solvent denaturation experiments on amphiphilic polymer **3** reveal a typical sigmoidal, i.e. cooperative, folding behavior (Figs. 3 and 4). When compared to shorter oligomers of similar structure [22,23], similar solvent titration curves are observed having a slightly shifted transition point indicating a more stable helix as predicted by the helix-coil model [29]. However for reasons yet unknown, the transition does not appear to be sharpened. Both UV–vis as well as fluorescence spectroscopy in THF at 40 °C (GPC conditions) suggest

major population of the helical, i.e. compact, conformation and therefore the molecular weight determined by GPC most likely represents a lower limit.

3.3. Backbone crosslinking

In order to lock the helical structure, multiple dimeric crosslinks were introduced via topochemically controlled [2+2]photodimerization events between stacking cinnamate

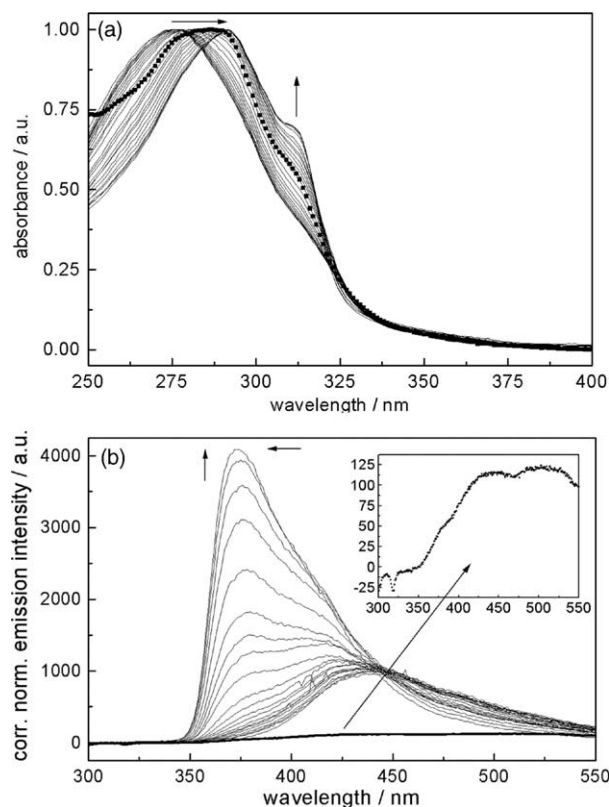


Fig. 3. Solvent denaturation experiments: (a) UV–vis absorption spectra of **3** recorded in acetonitrile with increasing chloroform content (100% $CH_3CN \rightarrow 100\% CHCl_3$ with increments according to Fig. 4 spectra were measured at similar concentration and have been normalized with respect to their maximum intensity) and **4** in 100% $CHCl_3$ (dotted line); (b) corrected and normalized fluorescence spectra of **3** recorded in acetonitrile with increasing chloroform content (100% $CH_3CN \rightarrow 100\% CHCl_3$ with increments according to Fig. 4 and **4** in 100% $CHCl_3$ (dotted line and inset).

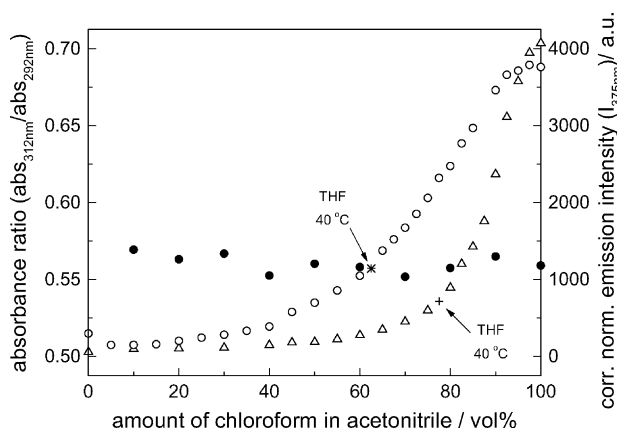


Fig. 4. Plots of UV-vis absorbance ratio ($\text{abs}_{312\text{nm}}/\text{abs}_{292\text{nm}}$) and normalized fluorescence intensity ($I_{375\text{nm}}$), respectively, as a function of the volume percent chloroform in acetonitrile (25 °C): UV-vis of **3** (○), fluorescence of **3** (△), UV-vis of **4** (●). Also shown: UV-vis of **3** in THF at 40 °C (*) and fluorescence of **3** in THF at 40 °C (+).

moieties [30,31]. For this purpose, polymer **3** was irradiated under high dilution conditions in the folding promoting solvent acetonitrile (Fig. 2). Monitoring the smoothly decreasing UV-vis absorbance and the corresponding extinction difference analysis indicate clean photoconversion of the cinnamate moieties. After 20 min of irradiation, the resulting crosslinked polymer **4** was again subjected to an UV-vis titration experiment (Figs. 3a and 4). No significant spectral changes were observed with increasing amount of the denaturant chloroform [32] thereby clearly

demonstrating the locked helical conformation. The slightly higher absorbance ratio ($\text{abs}_{312\text{nm}}/\text{abs}_{292\text{nm}}$) is attributed to some degree of structural reorganization during crosslinking as independently supported by the fluorescence spectrum of **4** in chloroform (Fig. 3b). While the almost negligible emission band (Fig. 3b inset) is reminiscent of the folded “pseudoexcimer” **3**, the much lower emission intensity can be explained by the diminished π,π -overlap in **4** due to geometrical changes introduced by photodimerization.

Molecular mechanics calculations point to the introduction of a considerable tilt angle of $\sim 30^\circ$ while the distance between the π -systems remains constant during the crosslinking process (Fig. 5a). In accordance with the topochemical principle [31], the helical structure should favor the formation of β -truxinates **5**, i.e. *syn* head-head photodimers, since they introduce the least conformational changes during the crosslinking event. Structural evidence for the proposed stereochemistry of **5** arises from NMR spectroscopy (Fig. 5b) due to the diagnostic doublet at $\delta = 4.0$ ppm [33]. In addition, the up-field shifted signal of the residual vinyl protons provides additional support for the locked helical structure [22,27] and allows a rough estimation of the degree of crosslinking amounting to ca. 20–30%, which is in reasonable agreement with the UV-vis absorption decrease during the course of irradiation.

As expected, GPC analysis shows that short irradiation times favor formation of mainly intramolecularly crosslinked polymers, while extensive irradiation leads to additional intermolecular crosslinking. Performing the crosslinking reaction in a denaturant such as chloroform, a polymer with high

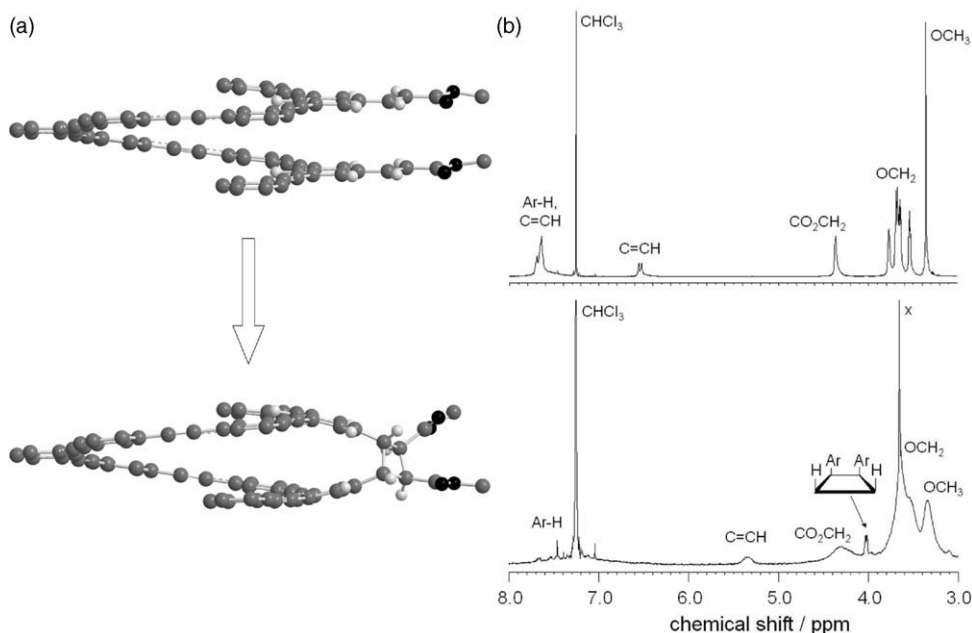


Fig. 5. Topochemical crosslinking control: (a) MM2 optimized molecular models of two π,π -stacking crosslinking units in **3** showing one parallel, stacked cinnamate pair with a 3.4 Å distance before irradiation (top) and its resulting β -truxinate (*syn* head-head photodimer) after irradiation still exhibiting a 3.4 Å distance between the centers of the phenyl rings that are however tilted by 30.5° (bottom). For clarity, the side chains and hydrogen atoms of the helical backbone have been omitted. (b) ¹H NMR spectral comparison (CDCl₃, 23 ± 2 °C) of polymer **3** (top) and its crosslinked derivative **4** after 20 min irradiation (bottom).

degree of intermolecular crosslinks and *transoid* conformations was formed.

4. Conclusions

Here, we have shown the covalent stabilization of a hollow helical conformation and therefore demonstrating the feasibility of our novel approach to organic nanotubes (Fig. 1). Utilizing this concept, organic nanotubes of controlled dimensions as well as specific local surface functionality should ultimately be realized.

Acknowledgments

Generous support by the Sofja Kovalevskaja Award of the Alexander von Humboldt Foundation, endowed by the Federal Ministry of Education and Research (BMBF) within the Program for Investment in the Future (ZIP) of the German Government, is gratefully acknowledged.

References

- [1] Nanotechnology, *Sci. Am.* (special issue) 285 (3) (2001).
- [2] Committee on Challenges for the Chemical Sciences in the 21st Century of the National Research Council, *Beyond the Molecular Frontier*, National Academy Press, New York, 2003.
- [3] S. Hecht, *Angew. Chem. Int. Ed.* 42 (2003) 24.
- [4] J.-M. Lehn, *Supramolecular Chemistry: Concepts and Perspectives*, VCH, Weinheim, 1995.
- [5] Supramolecular chemistry and self-assembly, *Science* (special issue) 295 (2002) 2400.
- [6] F. Cacialli, P. Samori, C. Silva, *Mater. Today* 7 (4) (2004) 24.
- [7] J.K. Strosio, D.M. Eigler, *Science* 254 (1991) 1319.
- [8] Ph. Avouris, *Acc. Chem. Res.* 28 (1995) 95.
- [9] Ph. Avouris, *Sci. Am.* 282 (3) (2000) 62.
- [10] Y. Xia, P. Yang, Y. Sun, Y. Wu, B. Mayers, B. Gates, Y. Yin, F. Kim, H. Yan, *Adv. Mater.* 15 (2003) 353.
- [11] Carbon nanotubes, *Acc. Chem. Res.* (special issue) 35 (12) (2002).
- [12] A. Hirsch, *Angew. Chem. Int. Ed.* 41 (2002) 1853.
- [13] S.S. Wong, E. Joselevich, A.T. Woolley, C.L.C.M. Cheung, C.M. Lieber, *Nature* 394 (1998) 52, For the only notable exception see functionalization of the carbon nanotube's ends by oxidation to the corresponding terminal carboxylic acids:
- [14] D.T. Bong, T.D. Clark, J.R. Granja, M.R. Ghadiri, *Angew. Chem. Int. Ed.* 40 (2001) 988.
- [15] S. Hecht, M.A. Balbo Block, C. Kaiser, A. Khan, *Top. Curr. Chem.*, in press.
- [16] S. Hecht, A. Khan, *Angew. Chem. Int. Ed.* 42 (2003) 6021.
- [17] F. Li, S.I. Yang, Y. Ciringh, J. Seth, C.H. Martin, D.L. Singh, D. Kim, R.R. Birge, D.F. Bocian, D. Holten, J.S. Lindsey, *J. Am. Chem. Soc.* 120 (1998) 10001–10017.
- [18] D.R. Coulson, *Inorg. Syn.* 13 (1971) 121–124.
- [19] D.J. Hill, M.J. Mio, R.B. Prince, T.S. Hughes, J.S. Moore, *Chem. Rev.* 101 (2001) 3893.
- [20] T. Nakano, Y. Okamoto, *Chem. Rev.* 101 (2001) 4013.
- [21] J.J.L.M. Cornelissen, A.E. Rowan, R.J.M. Nolte, N.A.J.M. Sommerdijk, *Chem. Rev.* 101 (2001) 4039.
- [22] J.C. Nelson, J.G. Saven, J.S. Moore, P.G. Wolynes, *Science* 277 (1997) 1793.
- [23] K. Matsuda, M.T. Stone, J.S. Moore, *J. Am. Chem. Soc.* 124 (2002) 11836, Defined as a helix having 6 repeat units per turn as evidenced by ESR double spin labeling experiments:.
- [24] U.H.F. Bunz, *Chem. Rev.* 100 (2000) 1605, For a comprehensive review about poly(phenyleneethynylene)s, mostly of the *para*-type consult:.
- [25] A. Khan, S. Hecht, *Chem. Commun.* (2004) 300.
- [26] Y. Tobe, N. Utsumi, K. Kawabata, A. Nagano, K. Adachi, S. Araki, M. Sonoda, K. Hirose, K. Naemura, *J. Am. Chem. Soc.* 124 (2002) 5350.
- [27] S. Lahiri, J.L. Thompson, J.S. Moore, *J. Am. Chem. Soc.* 122 (2000) 11315.
- [28] R.B. Prince, J.G. Saven, P.G. Wolynes, J.S. Moore, *J. Am. Chem. Soc.* 121 (1999) 3114.
- [29] B.H. Zimm, J.K. Bragg, *J. Chem. Phys.* 31 (1959) 526.
- [30] G.M.J. Schmidt, *Pure Appl. Chem.* 27 (1971) 647.
- [31] V. Ramamurthy, K. Venkatesan, *Chem. Rev.* 87 (1987) 433.
- [32] D.J. Hill, J.S. Moore, *Proc. Natl. Acad. Sci.* 99 (2002) 5053.
- [33] D.A. Ben-Efraim, B.S. Green, *Tetrahedron* 30 (1974) 2357.